AIAA 2000-0884

AN ARNOLDI APPROACH FOR GENERATION OF REDUCED-ORDER MODELS FOR TURBOMACHINERY

K.E. Willcox, J. Peraire, J. White
Massachusetts Institute of Technology
Cambridge, MA 02139

38th Aerospace Sciences Meeting & Exhibit
10-13 January 2000
Reno, Nevada

For permission to copy or republish, contact the American Institute of Aeronautics and Astronautics
1801 Alexander Bell Drive, Suite 500, Reston, VA 22091

AN ARNOLDI APPROACH FOR GENERATION OF REDUCED-ORDER MODELS FOR TURBOMACHINERY

K.E. Willcox*, J. Peraire†, J. White‡
Massachusetts Institute of Technology
Cambridge, MA 02139

Abstract

Linear reduced-order aerodynamic models are developed for aeroelastic analysis of turbomachines. Systematic model order reduction of a high-fidelity CFD method is performed to obtain low-order models which replicate the output behaviour of the CFD model over a restricted range of inputs. The reduced-space basis is constructed using a block Arnoldi method which provides an approximation of the high-fidelity system transfer function. Linearity of the governing equations is exploited to compute this basis efficiently. The aerodynamic model is cast in the time domain in state-space form and is coupled with a simple mass-spring-damper structural model. The reduction technique is applicable to viscous and three-dimensional problems, although here results are presented for two-dimensional, inviscid flow. In this case, the number of states of the model is on the order of ten per blade passage, making it appropriate for control applications. The use of generalised boundary conditions allows the models to be easily coupled to other engine components. This coupling is illustrated through analysis of a multi-stage problem.

Introduction

With the current trend towards increased operating speeds and more flexible blading, aeroelasticity has become a critical consideration in the design of compressors. Understanding and predicting aeroelastic phenomena are crucial to ensuring that a compressor will operate within stability boundaries, and thus has a large impact on the design process. Appropriate blade design, together with strategies for controlling the onset of instabilities, can significantly impact the stable operating range, potentially leading to better compressor performance. In addition, understanding high cycle fatigue is important to prolong engine lifetimes.

Aeroelasticity is concerned with the interaction between structural dynamics and aerodynamics. In the context of turbomachines, models must be developed which accurately describe the deformations of the bladed disks, and also the complicated flow through the engine. While the structural dynamics can typically be well represented by a linear analysis, it is generally agreed that the unsteady aerodynamic effects are extremely complex. At least some of the flow details (such as shock motion, blade loading, viscosity and boundary conditions) must be modelled to obtain realistic analyses. The current state of the art utilises CFD analyses to capture as much of the physics as possible, however such techniques are generally too computationally expensive to use for unsteady analyses, especially if the full rotor and more than one blade row need to be considered. More efficient methods for time-varying flow can be obtained if the disturbances are small, and the unsteady solution can be considered to be a small perturbation about a steady-state flow.[1] In this case, a set of linearised equations is obtained which can be time-marched to obtain the flow solution at each instant. However for control applications, any CFD-based technique will generate models with a prohibitively high number of states.

Instead, for aeroelastic analyses of turbomachines, the approach has typically been to use simplified aerodynamic models which can be incorporated into the aeroelastic framework in their entirety. The flow is usually assumed to be two-dimensional and potential. Efficient semi-analytic models for lightly loaded thin blades have been developed for subsonic flow[2] and for supersonic flow.[3] These methods are useful near design conditions but inadequately predict the flow off-design, as blade loading effects become important[4] and also do not exist for all flow regimes; in particular the modelling of transonic flows poses a difficulty. Often, the assumptions involved in deriving these simplified models further restrict their range of validity, for instance they may not be valid for high spatial frequency disturbances.[5]

Reduced-order modelling provides an attractive alternative means for obtaining suitable aeroelastic models and is now a well-developed technique for linear flow problems.[6] The basic idea is to project the

*Research Assistant, Department of Aeronautics and Astronautics
†Professor, Department of Aeronautics and Astronautics
‡Professor, Department of Electrical Engineering and Computer Science

Copyright ©2000 by Massachusetts Institute of Technology. Published by the American Institute of Aeronautics and Astronautics, Inc. with permission.

high-fidelity CFD solutions onto a set of basis functions which span the flow solution space efficiently. Models are obtained which replicate the high-fidelity aerodynamics of the CFD analysis over a restricted range of inputs, but which have only a few states. One possibility for a basis is to compute the eigenmodes of the system.[7,8] This can lead to efficient models and the eigenmodes themselves often lend physical insight to the problem. However, typical problem sizes are on the order of tens of thousands of degrees of freedom per blade passage even in two dimensions, and solution of such a large eigen-problem is in itself a very difficult task. The proper orthogonal decomposition technique (POD) has been developed as an alternate method of deriving the basis functions[9,10] and has been widely applied to many different problems including flow about an isolated airfoil.[11] An efficient frequency domain use of the POD has been developed for solution of turbomachinery flows.[12] Since the basis vectors are obtained from solutions of the system, the reduced-order model produced by the POD is only applicable to flows very similar to those considered in the construction of the model. This raises an issue if the model is to be applied in a control framework, as we expect the dynamics of the controlled and uncontrolled systems to differ significantly.[13]

In this paper an Arnoldi-based method is developed which provides an alternative to both the eigenmode and the POD approaches. The Arnoldi algorithm can be used to generate basis vectors which form an orthonormal basis for the Krylov subspace. The full set of Arnoldi vectors spans the same solution space as the system eigenvectors. An efficient reduced set can be constructed by considering both inputs and outputs of interest. Padé-based reduced-order models have been developed for linear circuit analysis using the Lanczos process.[14] This approach matches as many moments of the system transfer function as there are degrees of freedom in the reduced system. While the Arnoldi vectors match only half the number of moments as the Padé approximation, they preserve system definiteness and therefore often preserve stability.[15] Reduced-order models for the linearised potential flow about isolated airfoils have been derived using Arnoldi Ritz vectors.[16]

Generation of reduced-order models from the two-dimensional linearised Euler equations will be considered here, however the approach could be easily extended to three-dimensional and viscous models if the underlying CFD model were available. The model will be developed in the time domain and cast in state-space form, and the resulting reduced-order model will have roughly ten states per blade passage. Simulation in the time domain allows for arbitrary forcing to be considered. It also enables the aerodynamics to be easily incorporated within a global engine model or coupled to an active control model. The small size of the reduced-order model makes it amenable to control design and mistuning analyses, and also allows for the full rotor to be considered and for the analysis of multi-stage problems.

In this paper the underlying CFD model will be described, and some possibilities for model order reduction techniques will be discussed. The Arnoldi-based approach will be presented and compared to the POD approach. Model reduction results will be presented for a twenty-blade transonic rotor. The performance will be compared to both the linearised CFD simulation and the POD method. The aerodynamic reduced-order model will also be coupled to a simple structural model for each blade and the aeroelastic system stability and forced response investigated. Finally, the utility of the general input/output form of the models is demonstrated by considering analysis of a multiple blade row problem.

Aeroelastic Model

Figure 1 illustrates the concept of an aeroelastic model. We are often not concerned with the precise details of the flow field, but instead with predicting certain relevant output quantities accurately. These outputs are typically the forces and moments acting on the blades, and sometimes outgoing flow disturbances at the passage inlet and exit. The aerodynamic problem can be viewed as an input/output system where blade motions, incoming flow perturbations and flow operating conditions provide the inputs. Similarly, the structural model can be viewed as a means of obtaining the blade displacements and stresses given a specific forcing configuration. Computational models, such as finite element models for the structure and CFD models for the flow, should provide an accurate representation of the appropriate outputs given a set of input conditions. The operating conditions, an important input to the aerodynamic model, are represented by many different parameters (for example Mach number, rotation speed, pressure ratio), and so the aerodynamics constitute a complicated problem with many controlling parameters.

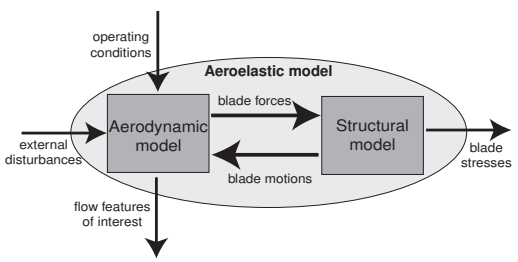

Fig. 1 Input/output view of aeroelastic model.

The system has associated to it a certain "state", which, along with the input, completely determines the behaviour and output characteristic. For example, for the structural system, the states may be the instantaneous deformations and motions of the blades, while

the aerodynamic states may be the values of the flow variables over the entire domain. The computational tools must provide a model of how the system states evolve with time due to certain forcing inputs. In general, we will consider a bladed disk with r deformable blades, operating at conditions represented by Θ. In addition, we will allow an external flow disturbance d. A general nonlinear model takes the form

$$\frac{d\mathbf{s}}{dt} = f(\mathbf{s}, \Theta, d, t) \qquad \mathbf{y} = g(\mathbf{s}, \Theta, d, t), \tag{1}$$

where $\mathbf{s}$ contains all the aerodynamic and structural states for the full bladed disk, and $\mathbf{y}$ contains all outputs of interest.

If we consider small blade deformations and small deviations of the aerodynamics from the mean operating conditions, then (1) can be linearised to obtain

$$\frac{d\mathbf{s}}{dt} = M(\overline{\Theta})\mathbf{s} + \sum_{\ell} \mathbf{E}_{\ell}(\overline{\Theta}) d_{\ell}, \tag{2}$$

where $M(\overline{\Theta})$ represents the linearisation of the unforced dynamics evaluated at the mean operating conditions, $\overline{\Theta}$, and $\mathbf{E}_{\ell}$ is the forcing vector corresponding to the ℓth spatial forcing mode. Since the dynamics are linear, we can always split any spatial disturbance into its spatial Fourier modes, compute the answer separately for each mode ℓ and sum over all ℓ at the end to recover the complete answer.

Nonlinear Aerodynamic Model

Consider an arbitrary two-dimensional time-varying control volume $\Omega(t)$ with boundary $\Gamma(t)$. The Euler equations governing the unsteady, two-dimensional flow of an inviscid compressible fluid can be written in integral form as

$$\frac{\partial}{\partial t} \int_{\Omega} W dx dy + \oint_{\Gamma} (F n_x + G n_y)\, d\Gamma = 0, \tag{3}$$

where n_x and n_y are the cartesian components of the unit normal vector pointing out of Ω, W is the unknown vector of conserved variables given by

$$W = (\rho, \rho u, \rho v, e)^T, \tag{4}$$

and F and G are the inviscid flux vectors given by

$$F = \begin{pmatrix} \rho(u - x_t) \\ p + \rho u(u - x_t) \\ \rho v(u - x_t) \\ pu + e(u - x_t) \end{pmatrix} G = \begin{pmatrix} \rho(v - y_t) \\ \rho u(v - y_t) \\ p + \rho v(v - y_t) \\ pv + e(v - y_t) \end{pmatrix}. \tag{5}$$

Here ρ, u, v, p, and e denote density, cartesian velocity components, pressure, and total energy, respectively. x_t and y_t are the speeds in the x and y directions with which the boundary $\Gamma(t)$ moves. Also, for an ideal gas the equation of state becomes

$$e = \frac{p}{\gamma - 1} + \frac{1}{2}\rho(u^2 + v^2), \tag{6}$$

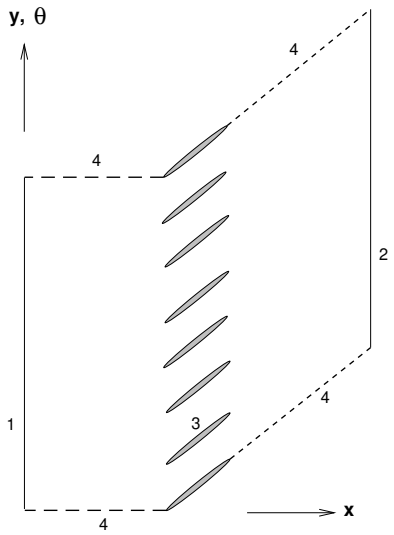

Fig. 2 Rectilinear two-dimensional representation of cascade. Inlet boundary (1), exit boundary (2), blade surfaces (3) and periodic boundaries (4).

where γ is the ratio of specific heats.

To obtain a rectilinear two-dimensional representation of the cascade, the rotor is unwrapped in the circumferential direction as shown in Figure 2. The boundaries extending upstream from the leading edge and downstream from the trailing edge of the blade surfaces are periodic boundaries. To preserve the circumferential nature of the physical problem, a condition is enforced that the flow along the upper periodic boundary is the same as that along the lower periodic boundary. The governing equations are discretised using a finite volume formulation on an unstructured triangular grid covering this computational domain and approximations to the unknown flow vector W are sought at the vertices of that grid. At boundary vertices, some of the flow variables are prescribed via appropriate boundary conditions. These prescribed quantities are contained within the vector $\mathbf{U}_b$, while the remaining unknown flow quantities are contained in the vector $\mathbf{U}$. For interior nodes the components of the unknown vector $\mathbf{U}$ are the conservative flow variables (4), while for boundary nodes a transformation to other appropriate flow quantities is performed. The particular transformation depends on which flow quantities are specified via the boundary conditions at that node. The spatial discretisation, along with appropriate variable transformations, leads to a large set of nonlinear ordinary differential equations for the unknown flow vector $\mathbf{U}$, which can be written as

$$\frac{d\mathbf{U}}{dt} + \mathbf{R}(\mathbf{U}, \mathbf{U}_b, \mathbf{x}) = 0, \tag{7}$$

where $\mathbf{R}(\mathbf{U}, \mathbf{U}_b, \mathbf{x})$ represents the nonlinear flux contributions which are a function of the problem geometry $\mathbf{x}$, the flow solution $\mathbf{U}$ and the boundary conditions $\mathbf{U}_b$.

We consider unsteady motion in which each blade can move with two degrees of freedom, although in general, blade shape deformations could also be included. For blade i the bending displacement (plunge) is denoted by h_i and torsion about an elastic axis (pitch) by α_i. At the passage inlet and exit we allow external flow disturbances. These could be, for example, time-varying pressure or velocity distortions which may be due to a neighbouring blade row or to an inhomogeneity in the incoming flow. Given blade motion $\mathbf{q}$ and disturbance $\mathbf{d}$, the boundary conditions can be written as

$$\mathbf{U}_b = \mathbf{U}_p(\mathbf{q}, \dot{\mathbf{q}}, \mathbf{d}, \mathbf{x}), \tag{8}$$

where $\mathbf{q}$ is a vector containing the plunge and pitch displacements for each blade

$$\mathbf{q}_i = [h_i \ \alpha_i]^T. \tag{9}$$

Linearised Aerodynamic Model

Steady-state solutions can be evaluated by driving the nonlinear residual $\mathbf{R}(\mathbf{U}, \mathbf{U}_b, \mathbf{x})$ in (7) to zero. However, to integrate the full nonlinear equation in time for unsteady flows is computationally expensive, especially if the disturbances considered have circumferential variation. If we limit ourselves to the consideration of small amplitude unsteady motions, the problem can be considerably simplified by linearising the equations. We assume that the unsteady flow and grid geometry are small perturbations about a steady state

$$\begin{aligned} \mathbf{U}(\mathbf{x}, t) &= \overline{\mathbf{U}}(\mathbf{x}) + \mathbf{U}'(\mathbf{x}, t) \\ \mathbf{U}_b(\mathbf{x}, t) &= \overline{\mathbf{U}}_b(\mathbf{x}) + \mathbf{U}'_b(\mathbf{x}, t) \\ \mathbf{x}(t) &= \overline{\mathbf{x}} + \mathbf{x}'(t). \end{aligned} \tag{10}$$

Additionally, we assume that the unsteady forcing terms $\mathbf{q}$, $\dot{\mathbf{q}}$ and $\mathbf{d}$ are small. Performing a Taylor expansion about steady-state conditions and neglecting quadratic and higher order terms in $\mathbf{U}'$, $\mathbf{U}'_b$ and $\mathbf{x}'$, the linearised form of equation (7) is

$$\frac{d\mathbf{U}'}{dt} + \frac{\partial \mathbf{R}}{\partial \mathbf{U}}\mathbf{U}' + \frac{\partial \mathbf{R}}{\partial \mathbf{U}_b}\mathbf{U}'_b + \frac{\partial \mathbf{R}}{\partial \mathbf{x}}\mathbf{x}' = 0, \tag{11}$$

where all derivatives are evaluated at steady-state conditions. Note that due to the linear assumption, the grid is not actually deformed for unsteady calculations, however the final term on the left-hand side of equation (11) represents the first order effects of grid motion. Likewise, the boundary conditions can be linearised to obtain

$$\mathbf{U}'_b = \frac{\partial \mathbf{U}_p}{\partial \mathbf{q}}\mathbf{q} + \frac{\partial \mathbf{U}_p}{\partial \dot{\mathbf{q}}}\dot{\mathbf{q}} + \frac{\partial \mathbf{U}_p}{\partial \mathbf{d}}\mathbf{d} + \frac{\partial \mathbf{U}_p}{\partial \mathbf{x}}\mathbf{x}'. \tag{12}$$

We can further simplify the system by condensing $\mathbf{U}'_b$ out of (11) using (12) and writing the grid displacement as a linear function of blade displacement

$$\mathbf{x}' = \mathcal{T}\mathbf{q}, \tag{13}$$

where $\mathcal{T}$ is a constant transformation matrix. The final set of ordinary differential equations then becomes

$$\begin{aligned} \frac{d\mathbf{U}'}{dt} + \frac{\partial \mathbf{R}}{\partial \mathbf{U}}\mathbf{U}' = &\left(-\frac{\partial \mathbf{R}}{\partial \mathbf{x}}\mathcal{T} - \frac{\partial \mathbf{R}}{\partial \mathbf{U}_b}\frac{\partial \mathbf{U}_p}{\partial \mathbf{q}} - \frac{\partial \mathbf{R}}{\partial \mathbf{U}_b}\frac{\partial \mathbf{U}_p}{\partial \mathbf{x}}\mathcal{T}\right)\mathbf{q} \\ &- \frac{\partial \mathbf{R}}{\partial \mathbf{U}_b}\frac{\partial \mathbf{U}_p}{\partial \dot{\mathbf{q}}}\dot{\mathbf{q}} - \frac{\partial \mathbf{R}}{\partial \mathbf{U}_b}\frac{\partial \mathbf{U}_p}{\partial \mathbf{d}}\mathbf{d}, \end{aligned} \tag{14}$$

which can be written equivalently as

$$\frac{d\mathbf{U}'}{dt} = A\mathbf{U}' + B\mathbf{u} + E\mathbf{d}. \tag{15}$$

Here $\mathbf{u} = [\mathbf{q} \ \dot{\mathbf{q}}]^T$ is the input vector containing the displacement and velocity of each blade, and the matrices B and E contain the appropriate terms of equation (14).

To determine the unsteady response of the cascade, the inputs $\mathbf{u}(t)$ and $\mathbf{d}(t)$ are specified and the large system (15) is time-marched to determine the resulting flow. Often we are not interested in obtaining the actual flow itself, but in relevant output quantities. These are typically the forces and moments acting on the blades, but could be any feature of the response. We define an output vector $\mathbf{y}$ as

$$\mathbf{y} = C\mathbf{U}' + D\mathbf{u}, \tag{16}$$

which for the analyses presented here contains the aerodynamic force and moment acting on each blade, and possibly also the outgoing flow perturbations at the passage inlet and exit. C and D are matrices containing the geometric and mean flow contributions to the output evaluation.

Reduction Using Congruence Transforms

While the CFD model described in the previous section provides an accurate representation of the flow aerodynamics, the set of ordinary differential equations obtained is extremely large, and is unsuitable for stability analysis or routine design calculations. By restricting the range of inputs over which the model is valid, systematic model order reduction can be performed to obtain a reduced-space basis. There are several options available for performing the reduction, a few of which will be outlined here. It is desirable to choose an orthogonal set of vectors, as the resulting congruent transformation preserves the system definiteness, and therefore often preserves system stability.

If the set of q orthonormal basis vectors are contained in the columns of the matrix V_q, a qth order approximation to the perturbation solution can be made by assuming

$$\mathbf{U}' = V_q\mathbf{z}, \tag{17}$$

where $\mathbf{z}(t)$ is the reduced-order aerodynamic state vector. Substituting this representation of $\mathbf{U}'$ into the

linearised governing equations (15) and premultiplying the system by V_q^T, we obtain the reduced-order system

$$\frac{d\mathbf{z}}{dt} = V_q^T A V_q \mathbf{z} + V_q^T B \mathbf{u} + V_q^T E \mathbf{d}. \qquad (18)$$

Writing the reduced-order matrix as $A_r = V_q^T A V_q$, it is clear from (18) that the definiteness of the original system has been preserved. This can be seen by considering an arbitrary vector $\mathbf{v}$, then

$$\mathbf{v}^T A_r \mathbf{v} = \mathbf{v}^T V_q^T A V_q \mathbf{v} = (V_q \mathbf{v})^T A (V_q \mathbf{v}). \qquad (19)$$

Therefore if the original matrix A yields strictly negative results from a quadratic form such as (19), so will the reduced system matrix A_r. A negative semidefinite matrix implies that all the eigenvalues have nonpositive real part and the aerodynamic system is stable. In this case, if the original system is stable, so will be the reduced-order model. We note that this property is not preserved in transforms of the form $A_r = W_q^T A V_q$ where W_q and V_q are bi-orthogonal.

Eigenmode Representation

An obvious choice might be to compute the eigenmodes of the large matrix A and to form the basis with the eigenvectors whose eigenvalues fall within the frequency range of interest. This approach has been taken for many problems, especially in structural dynamics where the matrices are generally symmetric and the eigenmodes are easy to compute. In fluid problems however, the eigenmodes of the very large matrix A are much more difficult to compute. Even in two dimensions it was found that for the full Euler equations the matrix was badly conditioned and that the eigenmodes suffered from non-normality problems. If only a few eigenmodes are needed, then Arnoldi methods can be used to compute the basis. However, static corrections must be included in the model to account for the excluded modes.[8]

Proper Orthogonal Decomposition

The POD is a popular alternative to the eigenmode approach for determining a reduced-space basis. Typically, a time simulation of the system for a characteristic unsteady flow is performed and instantaneous solutions or snapshots are obtained at selected times. These snapshots are then combined to produce an orthogonal set of basis vectors which represents the solution $\mathbf{U}'$ in some optimal way. More specifically, the basis vectors $\mathbf{\Psi}$ are chosen so as to maximise the following cost:[9]

$$\max_{\mathbf{\Phi}} \frac{\langle |(\mathbf{U}', \mathbf{\Phi})|^2 \rangle}{(\mathbf{\Phi}, \mathbf{\Phi})} = \frac{\langle |(\mathbf{U}', \mathbf{\Psi})|^2 \rangle}{(\mathbf{\Psi}, \mathbf{\Psi})}, \qquad (20)$$

where $(\mathbf{U}', \mathbf{\Psi})$ denotes the scalar product of the basis vector with the field $\mathbf{U}'(\mathbf{x}, t)$ and $\langle\ \rangle$ represents a time-averaging operation.

A POD approach to developing reduced-order models for turbomachinery problems has been developed by the authors[12] and is summarised here. To avoid performing a time simulation of the large linearised system (15), the forcing is decomposed into spatial and temporal Fourier modes, and advantage is taken of the fact that the governing equations are linear to consider each of these modes separately.

Consider first the motion of r blades given by $\mathbf{u}(t) = [\mathbf{u}_1^T(t)\ \mathbf{u}_2^T(t)\ \ldots\ \mathbf{u}_r^T(t)]^T$. Due to the circumferential nature of the problem, there exist within this motion discrete allowable values of spatial frequency σ_j. Moreover, due to the discrete nature of the blades, the blade motion contains a finite number of spatial modes. For a bladed disk with r blades, there are just r possible modes, with spatial frequencies given by

$$\sigma_j = \frac{2\pi j}{r} \qquad j = 0, 1, 2, \ldots, r-1. \qquad (21)$$

Here, σ_j is known as the interblade phase angle and describes the phase difference between the motion of a given blade and its neighbour.[1]

A general motion of the blades $\mathbf{u}(t)$ can be decomposed into its spatial modes by performing a discrete Fourier transform. If we denote the complex magnitude of the modal component corresponding to σ_j by $\overline{\mathbf{u}}_j$, then for blade n we can write

$$\mathbf{u}_n(t) = Re\left\{ \sum_{j=0}^{r-1} \overline{\mathbf{u}}_j(t) e^{i(n-1)\sigma_j} \right\}. \qquad (22)$$

A similar decomposition can be performed for a general inlet or exit disturbance. Still the discrete values of σ_j defined by (21) are the only ones allowable (to satisfy circumferential periodicity), but now an infinite number of spatial modes may be present, that is j can take any integer value. The Fourier transform for a disturbance $\mathbf{d}$ can therefore be written

$$\mathbf{d}(t) = Re\left\{ \sum_{j=0}^{\infty} \overline{\mathbf{d}}_j(t) e^{i\sigma_j} \right\}. \qquad (23)$$

Similarly, the time-varying component of blade motion and disturbance forcing can be decomposed into temporal frequency components. In this case, an infinite number of possible frequencies exists. In practice, discrete values of temporal frequency are chosen, so that the blade motion can be represented as a summation over temporal and spatial modes. If m temporal frequencies are selected, then the motion of blade n can be written as

$$\mathbf{u}_n(t) = Re\left\{ \sum_{k=1}^{m} \sum_{j=0}^{r-1} \overline{\mathbf{u}}_{jk} e^{i(\omega_k t + (n-1)\sigma_j)} \right\}. \qquad (24)$$

A similar expression can be written for the disturbance. With m temporal frequencies and l spatial

frequencies, we obtain

$$\mathbf{d}(t) = Re\left\{\sum_{k=1}^{m}\sum_{j=0}^{l-1}\overline{\mathbf{d}}_{jk}e^{i(\omega_k t+\sigma_j)}\right\}. \qquad (25)$$

Assuming decompositions of the form (24) and (25) have been performed on the forcing functions, we can now consider each modal component separately. Consider then a blade motion $\mathbf{u}^{jk}$ containing a single temporal frequency ω_k and single spatial frequency σ_j. The motion of any blade n can be written in terms of the motion of the first blade as

$$\mathbf{u}_n^{jk}(t) = \overline{\mathbf{u}}_1^{jk}(t)e^{i\omega_k t}e^{i(n-1)\sigma_j}. \qquad (26)$$

The corresponding flow solution in each passage will also be harmonic of the form

$$\mathbf{U}_n^{jk}(t) = \overline{\mathbf{U}}_1^{jk}e^{i\omega_k t}e^{i(n-1)\sigma_j}, \qquad (27)$$

with the same spatial frequency σ_j because all blades have the same aerodynamic shape and so the jth spatial forcing only excites the jth spatial aerodynamic response. Here the vector $\mathbf{U}_n$ represents the unknown perturbation flow variables associated with blade n. Since each $\overline{\mathbf{U}}^{jk}$ contains a single spatial frequency, if the response of the first blade is known, then the response of all subsequent blades can be determined by using (27). The governing equations can therefore be discretised on a single blade passage making the computation much more efficient than a time domain calculation.

Analogous relations can be written for each modal component of $\mathbf{d}$, and the linearised Euler equations (15) can now be cast in the frequency domain on a single passage as

$$[i\omega_k - A_j]\,\overline{\mathbf{U}}_1^{jk} = B\overline{\mathbf{u}}_1^{jk} + E\overline{\mathbf{d}}_1^{jk}, \qquad (28)$$

where A_j represents the original matrix A for just one passage, but modified to allow for a complex periodicity condition. This condition enforces the fact that the flow along the upper periodic boundary is the same as that along the lower periodic boundary but phase shifted by the spatial frequency σ_j.

Resulting solutions of the frequency domain CFD equations (28) provide an image of the flow at each temporal frequency ω_k, for each spatial frequency σ_j. The real and imaginary parts of this image form the snapshots for the POD analysis. Although far more efficient than a POD analysis in the time domain, this approach requires the factorisation of the matrix $[i\omega_k - A_j]$ for each pair of frequencies. For a typical bladed disk, the cost of generating the snapshots can be high if a large frequency range is to be considered. Another issue with the POD approach is that it is necessary to arbitrarily specify a set of sample frequencies. Typically some knowledge will be available on the range of frequencies expected to be present in the system response, and the POD will be sampled over this range. However, it is also necessary to choose exactly which frequencies will be sampled within this range. If samples are placed too far apart, important system dynamics may be missed; if they are placed too closely together, a large number of matrix factorisations and solves is necessary and so the cost of generating the model becomes high.

Arnoldi-Based Model Order Reduction

An approach which contains some flavour of both the eigenmode and POD methods is developed in this section. While the basis is easy to compute, some of the issues associated with the sampling requirements in the POD are addressed. Our basic goal is to obtain a reduced system which has many fewer states than the original system, can be computed with a reasonable cost, but which still represents the original system's dynamics accurately. One approach to ensuring accurate representation of system dynamics is to try to match the transfer functions of the reduced and the original systems. Consider first a single input, single output system

$$\dot{\mathbf{U}}' = A\mathbf{U}' + \mathbf{b}u, \qquad y = \mathbf{c}^T\mathbf{U}', \qquad (29)$$

where we are considering only the portion of the output $\mathbf{y}$ which depends directly on the perturbation flow solution $\mathbf{U}'$. The direct transmission term in (16) does not affect the model order reduction procedure. The transfer function between input $u(t)$ and output $y(t)$ is then

$$H(s) = \mathbf{c}^T(sI - A)^{-1}\mathbf{b}, \qquad (30)$$

which can also be represented as a rational function

$$H(s) = \frac{N(s)}{D(s)} = \frac{b_{n-1}s^{n-1} + \ldots + b_1 s + b_0}{a_n s^n + \ldots + a_1 s + 1}, \qquad (31)$$

where n is the dimension of the high-order system (29). A qth order Padé approximation to the transfer function is obtained by retaining the first q coefficients in each of the polynomials $N(s)$ and $D(s)$ as follows:

$$H_q(s) = \frac{b_{q-1}s^{q-1} + \ldots + b_1 s + b_0}{a_q s^q + a_{q-1}s^{q-1} + \ldots + a_1 s + 1}. \qquad (32)$$

We also note that by retaining these $2q$ coefficients in the rational approximation, we in fact match the coefficients of the first $2q$ terms in a McLaurin expansion of the transfer function (30). We can write

$$H(s) = -\sum_{k=0}^{\infty} m_k s^k, \qquad (33)$$

where

$$m_k = \mathbf{c}^T A^{-(k+1)}\mathbf{b} \qquad (34)$$

is the kth moment of $H(s)$. A qth order Padé approximation can be constructed via the Lanczos process and will therefore match the first $2q$ moments of $H(s)$.[14]

An alternative approach is to use the Arnoldi method to generate a set of vectors which spans the qth order Krylov subspace defined by

$$\mathcal{K}_q(A, \mathbf{b}) = \text{span}\{A^{-1}\mathbf{b}, A^{-2}\mathbf{b}, ..., A^{-q}\mathbf{b}\}. \quad (35)$$

By selecting the sequence of vectors

$$\begin{aligned} \mathbf{\Psi}_1 &= A^{-1}\mathbf{b} \\ \mathbf{\Psi}_2 &= A^{-2}\mathbf{b} \perp \mathbf{\Psi}_1 \\ &\vdots \\ \mathbf{\Psi}_q &= A^{-q}\mathbf{b} \perp (\mathbf{\Psi}_1, \mathbf{\Psi}_2, \ldots, \mathbf{\Psi}_{q-1}), \end{aligned} \quad (36)$$

a basis is obtained which matches the first q moments of the system transfer function, that is half the number matched by the Padé approximation. However, since the Arnoldi approach is a congruent transformation, in many cases it generates models with guaranteed stability. It is possible to reduce systems with multiple inputs using the block Arnoldi method. For example, if we consider a system with two inputs u_1 and u_2,

$$\dot{\mathbf{U}}' = A\mathbf{U}' + \mathbf{b}_1 u_1 + \mathbf{b}_2 u_2, \quad (37)$$

then the block Arnoldi method is used to generate vectors which span the Krylov subspace

$$\begin{aligned} \mathcal{K}_q(A, \mathbf{b_1}, \mathbf{b_2}) = \text{span}\{&A^{-1}\mathbf{b}_1, A^{-1}\mathbf{b}_2, A^{-2}\mathbf{b}_1, \\ &A^{-2}\mathbf{b}_2, ..., A^{-q}\mathbf{b}_1, A^{-q}\mathbf{b}_2, \}. \end{aligned} \quad (38)$$

We also note that it is not necessarily the first q moments which must be matched. If we were to consider a Taylor series expansion of the transfer function about some non-zero value of s, a model could be obtained which would give a better approximation of the system dynamics for higher frequencies.[17]

In order to calculate the basis, we consider input vectors which correspond to a particular blade having a unit displacement or velocity and all other blades fixed. Although vectors must be constructed for each of the r blades being perturbed in turn, the calculation need only be performed once, with the remaining $r-1$ vectors constructed through symmetry considerations. Once again, we can use linearity to decompose this forcing into a set of orthogonal modes each containing a single spatial frequency, and the calculation for each of these modes can be performed on a single blade passage. For expansions of the transfer function about $s = i\omega_k$, solutions of the complex frequency domain equations (28) must be obtained. Further simplification can be obtained by noting that for expansions about $s = 0$, the set of Arnoldi vectors for spatial frequencies σ and $-\sigma$ are complex conjugates of one another.

Given the set of basis vectors $V_q = [\mathbf{\Psi}_1 \mathbf{\Psi}_2 ... \mathbf{\Psi}_q]$, we substitute the projection of $\mathbf{U}'$ (17) into the governing equations (15) and (16) to obtain the reduced-order system (18) which can be written as

$$\frac{d\mathbf{z}}{dt} = A_r\mathbf{z} + B_r\mathbf{u} + E_r\mathbf{d}, \qquad \mathbf{y} = C_r\mathbf{z} + D_r\mathbf{u}. \quad (39)$$

One can see the similarities between the POD approach and the multiple frequency point Arnoldi method. In fact, solving the system (28) at J frequencies to obtain the POD snapshots results in an identical data set as taking J frequency points and computing a single Arnoldi vector at each point (the subsequent orthogonalisation procedure differs between the two methods). This can be seen by noting that the vector which solves the complex system (28) is both the POD snapshot at the frequency ω_k and the first vector in the Arnoldi basis expanded about ω_k. It is postulated that very efficient models could be constructed by considering a range of frequencies and using the POD analysis to choose the basis vectors, but also computing more than one vector at each frequency as in the Arnoldi approach. One must evaluate the relative gain in choosing a higher number of frequency points, since by far the most expensive part of the calculation is the factorisation of the matrix in solving the linear system. In the Arnoldi approach, the matrix is computed and factored just once for each ω_k and σ_j, but several vectors are obtained per factorisation. For the POD, a different matrix must be factored for every pair of snapshots, and moreover the number of snapshots typically exceeds the final number of basis vectors constructed by a significant amount.

Results

Aerodynamic Reduced-Order Model for Transonic Cascade

Reduced-order models have been developed for subsonic and transonic cascades operating with general unsteady blade motion. A DFVLR L030-4 transonic rotor which operates at a steady-state inlet Mach number of 0.82 was analysed in unsteady plunging motion for a twenty-blade configuration. Arnoldi basis vectors were computed for the interblade phase angles present in the twenty-blade configuration. For plunging motion there are two inputs per blade - the plunge position h and the plunge velocity $\dot{h}$. The reduced-order aerodynamic model was constructed and the eigenvalue spectrum of this system is shown in Figure 3. For the case shown, there are six states for the zero interblade phase angle case and ten states for all other interblade phase angles (twenty for each pair $\sigma, -\sigma$), giving a total of 196 states in the reduced-order model. Note that $\sigma = 0$ is a special case where the plunge position h has no effect, and fewer modes are required to accurately capture the dynamics. Comparatively, the CFD computational grid for twenty passages would

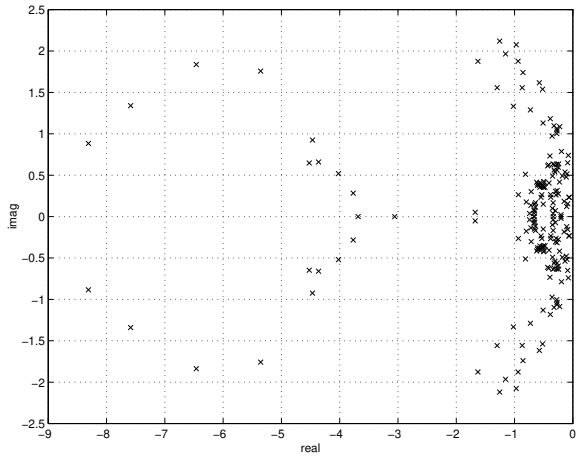

Fig. 3 Eigenvalue spectrum for Arnoldi reduced-order aerodynamic system. 6 states for $\sigma = 0°$, 10 states for all other σ (total 196 states).

have 71940 grid points, which corresponds to 287760 unknowns. Clearly a time-domain computation of this size is very expensive, however we will show that the cascade dynamics can be accurately captured with the above choice of less than two hundred states in the reduced-order model.

Forced response of the cascade to a pulse input is a good assessment of the model's capability, since a pulse contains a continuous spectrum of temporal frequencies. Comparison of reduced-order modelling predictions with results from the full simulation code (if these results were available) would determine how many modes are required to accurately capture the system dynamics. The input takes the form

$$h(t) = he^{-g(t-t_0)^2}, \tag{40}$$

where g is a parameter which determines how sharp the pulse is and thus the value of the highest significant frequency present.

As mentioned, it would be very expensive to perform a time simulation of the linearised CFD code on the full rotor. However if all blades are supplied with the same pulse input, a motion results in which only an interblade phase angle of zero is present and which can be solved using the linearised simulation code with just a single passage. The resulting non-dimensional vertical component of force on each blade as a function of time is depicted in Figure 4. It shows that excellent agreement is obtained with only a handful of states in the reduced-order model. This same case was considered using a reduced-order model constructed with the POD technique.[12] The POD samples were made at ten equally spaced reduced frequencies over the range $k = 0 - 1.22$ for each interblade phase angle. This frequency range spans the important content of the pulse for a value of $g = 0.01$. The response calculated with the POD reduced-order model is also shown in Figure 4. Although the POD response is more accurate than the Arnoldi response with four modes, with six modes the Arnoldi model is very close to the linearised simulation response, while the POD slightly underpredicts the force at both peaks.

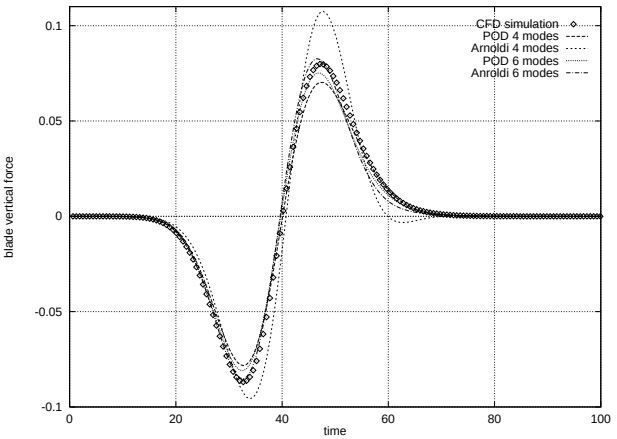

Fig. 4 Pulse response for Arnoldi and POD reduced-order models and linearised simulation code. $\sigma = 0°$, $g = 0.01$, $M = 0.82$.

For this problem, a total of two hundred matrix factorisations were performed to obtain the POD snapshots (ten sample frequencies for each of twenty interblade phase angles). In comparison, just eleven matrix factorisations were required for the Arnoldi reduced-order model since all vectors were computed about $s = 0$. The Arnoldi-based model is an order of magnitude cheaper to obtain than the POD model, and also does a better job of predicting the response. In addition, the POD reduced-order model is restricted to responses containing frequencies within the (arbitrary) sample range. The Arnoldi-based model contains no such restriction, although more modes will be required if flows containing higher frequencies are to be modelled. In this case, one might choose to use a multiple frequency point method as described earlier. The reduced-order models obtained using the POD method are very sensitive to the choice of sample frequencies. As mentioned previously, it is necessary to ensure not only that the correct range is sampled, but also that enough samples are performed over this range, or the system dynamics will not be accurately captured. Because more than one vector is computed at each frequency in the Arnoldi method, the dynamics can be captured without considering many frequency points (one can liken the Arnoldi approach to computing higher-order "derivatives" at each frequency point). An appropriate choice of frequency points for the Arnoldi method can reduce the required size of the reduced-order models, but is not necessarily required to capture system dynamics, as the example presented here demonstrates.

Structural Coupling

In the aeroelastic system (2), we also require a model which describes the evolution of the structural states. The structural model could be a complicated system (for example a reduced-order structural model derived from a finite element analysis[18]) or a simple model (for example a very low-order mass-spring model). We consider here a simple mass-spring-damper structural model where each blade can move in plunging motion with a natural frequency of ω_h. For plunge only, the structural equations of motion for each blade with mass m and chord c can be written as

$$\frac{d}{dt}\begin{bmatrix} h_j \\ \dot{h}_j \end{bmatrix} = \begin{bmatrix} 0 & 1 \\ -(kM)^2 & -2kM\zeta \end{bmatrix}\begin{bmatrix} h_j \\ \dot{h}_j \end{bmatrix} + \begin{bmatrix} 0 \\ \frac{2M^2}{\pi\mu} \end{bmatrix} C_l^j. \tag{41}$$

or in matrix form,

$$\dot{\mathbf{u}} = S\mathbf{u} + T\mathbf{y}. \tag{42}$$

In the above, the reduced frequency is defined in terms of the plunge natural frequency $k = \frac{\omega_h c}{V}$, ζ is the structural damping coefficient and $\mu = \frac{4m_i}{\pi\rho c^2}$ is the blade mass ratio. $C_l^j = y_j$ is the lift coefficient for blade j, and M and V are the inlet Mach number and axial velocity respectively. This structural model is then coupled to the aerodynamic reduced-order state-space system (39). The coupled system is as follows :

$$\begin{bmatrix} \dot{\mathbf{z}} \\ \dot{\mathbf{u}} \end{bmatrix} = \begin{bmatrix} A_r & B_r \\ TC_r & S + TD_r \end{bmatrix}\begin{bmatrix} \mathbf{z} \\ \mathbf{u} \end{bmatrix} + \begin{bmatrix} E_r \\ 0 \end{bmatrix}\mathbf{d}. \tag{43}$$

At each timestep the structural and aerodynamic equations can thus be solved simultaneously to determine the blade forced response. The eigenvalues of (43) can be evaluated to assess the stability of the aeroelastic system.

A time-marching simulation of the coupled system with no external disturbance was run with $k = 0.25$ and $\zeta = 0$. An initial plunge displacement was applied to one of the blades, then the coupled structural and aerodynamic response for the entire rotor was computed. Figure 5 shows the resulting displacement and lift force for each blade. Clearly the disturbed blade (blade 3) exhibits the largest response. Beyond the two closest blades, the force generated in very small. The resulting motion is decaying, although slowly since the coupled system is lightly damped.

Multistage Analysis

To demonstrate the utility of the reduced-order models for coupling blade rows to other engine components, a compressor stage with a stator and a rotor is analysed. The airfoil coordinates represent the third stage of a four stage low-speed research compressor.[19] The test conditions are inlet Mach numbers of 0.165 and 0.123, and inlet flow angles of 59.3° and 47.3° in the rotor and stator respectively. The gap between the stator and rotor is 47.5% of the rotor chord. Both the rotor and stator are analyzed, assuming that the rotor

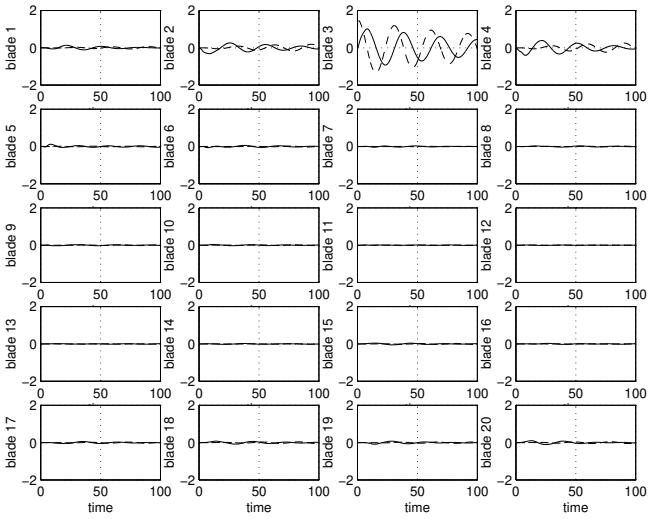

Fig. 5 Coupled system response to an initial plunge displacement input at blade 3 : blade displacement (dashed line) and blade lift force (solid line). $\mu = 100, k = 0.25, \zeta = 0$.

has 16 blades and the stator has 20. The actual compressor stage has 54 rotor blades and 74 stator vanes, but a smaller problem was chosen for analysis here. One quarter of the periodic domain (containing five stator vanes and four rotor blades) is shown in Figure 6, although the analysis is carried out on the full stage.

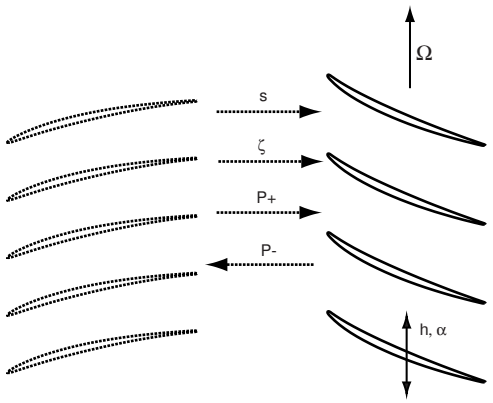

Fig. 6 Low-speed stator and rotor cross-sections.[19] Arrows represent the characteristic waves which allow communication between blade rows in multistage model: entropy wave (s), vorticity wave (ζ) and downstream and upstream running pressure waves ($P+$ and $P-$).

To create a multistage model, the rotating and stationary blade rows must be coupled. To accomplish this, reduced-order models are first developed in the relevant reference frame for each blade row. The models are then coupled in a time-marching simulation via the generalized boundary conditions which allow the reduced-order models for each blade row to communicate as shown in Figure 6. The results presented here are for reduced-order models of the rotor and stator with 248 and 118 aerodynamic states, respectively.

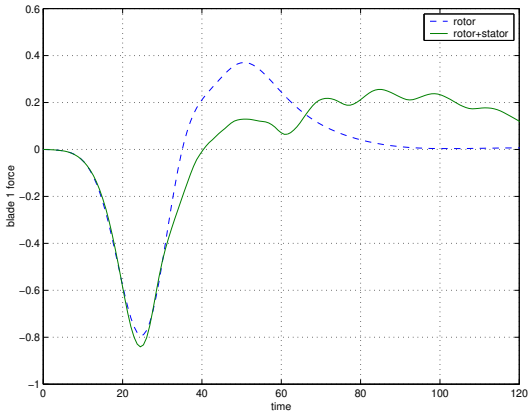

Fig. 7 Force on first rotor blade due to a prescribed pulse input in plunge displacement at second blade.

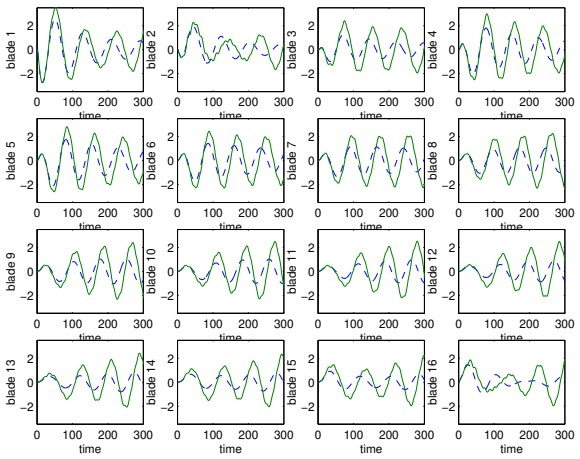

Fig. 8 Force on every blade of low speed rotor due to an initial displacement. Aeroelastic system with stator (solid lines) and rotor alone (dashed lines).

Because of the relative motion of the blade rows, the coupled reduced-order system is time varying and the coefficients of the aeroelastic system are periodic with the rotor rotation frequency. The usual definition of aeroelastic stability does not apply, since the system eigenvalues vary with time, however time marching the model allows the time-varying nature of the system to be examined. A crude stability analysis can also be performed by computing the frozen-time eigenvalues for a set of possible relative positions of the blade rows over one rotor revolution.

To investigate the effect of the stator on the rotor aerodynamics, the aerodynamic system was forced with a pulse input in plunge at the second blade and all other blades fixed. This motion excites all possible interblade phase angles in the rotor. The resulting lift forces on each of the rotor blades were calculated using both the rotor-alone reduced-order model and the coupled stator/rotor system. The response for the first blade is plotted in Figure 7. To give an indication of the time scales on this plot, we note that the non-dimensional period for one rotor revolution is $T_r = 316$. The solid line denotes the force calculated using the coupled model, while the dashed line is the force evaluated for the rotor alone. From Figure 7 we can see that the stator has a fairly significant effect. The magnitude of the peak response is roughly the same, but for the rotor-alone calculation, the force on the blade dies away smoothly as the pulse passes. With the stator included in the analysis, even after the pulse has passed through the system, we see oscillations due to the unsteady effect of the passing blades. These oscillations can be seen to have a period of approximately $T = 15$, which corresponds to one twentieth of the rotor revolution period.

The blade forces are next examined for the coupled aero-structural system with structural parameters $\mu = 100$, $k = 0.5$ and $\zeta = 0.13$. Figure 8 shows the response of the coupled system when the first blade is given an initial deflection. This initial condition excites all interblade phase angles simultaneously, so the response will evolve toward the least stable interblade phase angle as time proceeds. The decaying oscillations that exist for the rotor only become sustained oscillations due to the presence of the stator, with superimposed forces due to the stator passing. The time-varying aeroelastic matrix was evaluated at a series of time instants for the structural parameters described above, and the eigenvalues were determined. The loci of the structural eigenvalues are plotted as dots in Figure 9, while the crosses in this figure represent the positions of the structural eigenvalues for the rotor-alone system. The number above each eigenvalue denotes the number of nodal diameters associated to that eigenvector. The variations within the loci are small, however for some modes we notice a significant difference between the position of the locus and the rotor-alone structural eigenvalue. For almost all modes, the addition of the stator model is destabilising, which suggests that an isolated blade row analysis could significantly underpredict the response. The structural eigenvalue corresponding to $\ell = 15$ ($\sigma = 337.5°$) is barely stable for the rotor-alone system, however for the coupled system its locus lies entirely in the right half plane, and therefore accounts for the difference between the predicted responses in Figure 8. We therefore have the serious case that the rotor-alone predicts a barely stable system, but with the effect of the stator included the system is unstable.

Conclusions

A new method of producing reduced-order models for turbomachinery has been demonstrated. This method provides an excellent alternative to the eigenmode and POD approaches to reduced-order modelling. The basis vectors are constructed efficiently by applying the Arnoldi method to the frequency domain governing equations, while development of the model in the time domain allows for ease of coupling

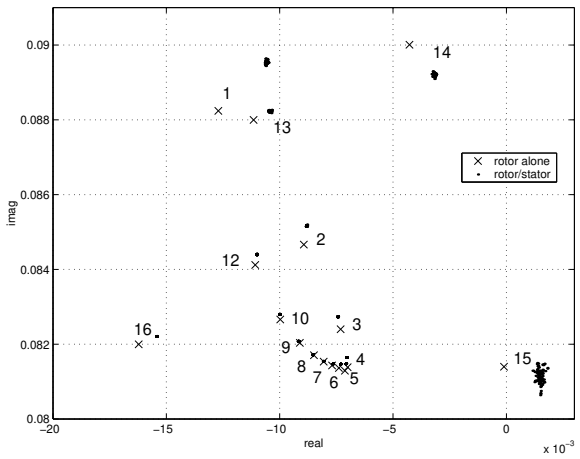

Fig. 9 Structural eigenvalues of aeroelastic system for low-speed rotor alone (crosses) and coupled stator/rotor (dots). Eigenvalues are numbered by their nodal diameter.

to actuation and control models and provides a convenient framework for integration within more global engine models. Preliminary analysis of a stator/rotor combination suggests that inter-blade row effects are significant and should be included if the aeroelastic response is to be predicted accurately. The framework developed is also particularly suited to the analysis of mistuned rotors where the interblade phase angles do not decouple and the entire rotor must be considered. It is also straightforward to extend this approach to viscous and three-dimensional flows if the underlying CFD model is available.

The Arnoldi basis has the benefits of an eigenmode approach in that it models the dynamics of the original high-order system, but it is much more straightforward to compute. The Arnoldi-based models are much cheaper to compute than those constructed using the POD since one matrix factorisation can be used to obtain many basis vectors, and are in general applicable to a wider range of flows. It is also possible to use Arnoldi methods with multiple frequency points to obtain efficient models which are valid for flows containing higher frequencies, however the models obtained are less sensitive than POD-based models to the choice of sample frequencies. In addition, outputs of interest can be included in the criterion for selecting the basis vectors, and further improvement can be obtained by post-processing the resulting reduced-order models using a truncated balanced realisation.

Acknowledgments

The authors wish to acknowledge helpful discussions with Dr. James Paduano. Support for this work has been provided by the AFOSR PRET program. J. Peraire and J. White also acknowledge the support of the Singapore MIT Alliance.

References

[1]Hall, K., *A Linearized Euler Analysis of Unsteady Flows in Turbomachinery*, Ph.D. thesis, Dept. of Aeronautics and Astronautics, MIT, May 1987.

[2]Whitehead, D., "Classical Two-Dimensional Methods," AGARD Manual on Aeroelasticity in Axial-Flow Turbomachines, Unsteady Turbomachinery Aerodynamics, Volume 1, 1987.

[3]Adamczyk, J. and Goldstein, M., "Unsteady Flow in a Supersonic Cascade wuth Subsonic Leading-Edge Locus," *AIAA Journal*, Vol. 16, No. 12, September 1978, pp. 1248–1254.

[4]Verdon, J., "Review of Unsteady Aerodynamic Methods for Turbomachinery Aeroelastic and Aeroacoustic Applications," *AIAA Journal*, Vol. 31, No. 2, February 1993, pp. 235–250.

[5]Moore, F. and Greitzer, E., "A Theory of Post-Stall Transients in Axial Compression Systems: Part I - Development of Equations," *Journal of Engineering for Gas Turbines and Power*, Vol. 108, January 1986, pp. 68–76.

[6]Dowell, E., Hall, K., Thomas, J., Florea, R., Epureanu, B., and Heeg, J., "Reduced Order Models in Unsteady Aerodynamics," AIAA Paper 99-1261, 1999.

[7]Hall, K., "Eigenanalysis of Unsteady Flows About Airfoils, Cascades and Wings," *AIAA Journal*, Vol. 32, No. 12, December 1994, pp. 2426–2432.

[8]Hall, K., Florea, R., and Lanzkron, P., "A Reduced Order Model of Unsteady Flows in Turbomachinery," ASME Paper 94-GT-291, 1994.

[9]Sirovich, L., "Turbulence and the Dynamics of Coherent Structures. Part 1 : Coherent Structures," *Quarterly of Applied Mathematics*, Vol. 45, No. 3, October 1987, pp. 561–571.

[10]Berkooz, G., Holmes, P., and Lumley, J., "The Proper Orthogonal Decomposition in the Analysis of Turbulent Flows," *Annual Review of Fluid Mechanics*, Vol. 25, 1993, pp. 539–575.

[11]Romanowski, M., "Reduced Order Unsteady Aerodynamic and Aeroelastic Models using Karhunen-Loéve Eigenmodes," AIAA Paper 96-194, 1996.

[12]Willcox, K., Paduano, J., Peraire, J., and Hall, K., "Low Order Aerodynamic Models for Aeroelastic Control of Turbomachines," AIAA Paper 99-1467, 1999.

[13]Tang, K., Graham, W., and Peraire, J., "Active Flow Control Using a Reduced Order Model and Optimum Control," AIAA Paper 96-1946, 1996.

[14]Feldmann, P. and Freund, R., "Efficient Linear Circuit Analysis by Padé Approximation via the Lanczos Process." *IEEE Transactions on Computer-Aided Design of Integrated Circuits and Systems*, Vol. 14, 1995, pp. 639–649.

[15]Silveira, L., Kamon, M., Elfadel, I., and White, J., "A Coordinate-Transformed Arnoldi Algorithm for Generating Guaranteed Stable Reduced-Order Models of RLC Circuits." *Computer Methods in Applied Mechanics and Engineering*, Vol. 169, No. 3-4, February 1999, pp. 377–389.

[16]Florea, R., Hall, K., and Dowell, E., "Eigenmode Analysis and Reduced Order Modeling of Unsteady Transonic Full Potential Flow Around Isolated Airfoils," Presented at the CEAS/AIAA/ICASE/NASA Langley International Forum on Aeroelasticity and Structural Dynamics, Williamsburg, VA, June 22-25, 1999.

[17]Grimme, E., *Krylov Projection Methods for Model Reduction*, Ph.D. thesis, Coordinated-Science Laboratory, University of Illinois at Urbana-Champaign, 1997.

[18]Ottarsson, G., Castanier, M., and Pierre, C., "A Reduced-Order Modeling Technique for Mistuned Bladed Disks," Proceedings of the 35th AIAA/ASME/ASCE/AHS/ASC Structures, Structural Dynamics, and Materials Conference, 1994.

[19]Silkowski, P., "Measurements of Rotor Stalling in a Matched and Mismatched Compressor," GTL Report 221, MIT, April 1995.